

X-ray Holography for Structural Imaging

D. V. Novikov,^{a*} B. Adams,^a T. Hiort,^a E. Kossel,^b G. Materlik,^a R. Menk^c and A. Walenta^c

^aHamburger Synchrotronstrahlungslabor HASYLAB am Deutschen Elektronen-Synchrotron DESY, Notkestr. 85, D-22607 Hamburg, Germany, ^bInstitut für Experimentalphysik, Universität Hamburg, Luruper Chaussee 149, D-22671 Hamburg, Germany, and ^cUniversität Gesamthochschule Siegen, Adolf-Reichweinstr. 2, D-57068 Siegen, Germany.
E-mail: novikov@desy.de

(Received 4 August 1997; accepted 22 December 1997)

X-ray atomic resolution holography is a new method for direct evaluation of three-dimensional electron density distribution in solids. The practical implementation of the multiple-energy technique on a synchrotron radiation source as well as image reconstruction from the experimental data are described. Holograms at several different energies were processed together to suppress twin images and artifacts from long-range-order effects in the experimental data sets. Reconstructed images of copper atoms in Cu₂O crystals are presented.

Keywords: imaging; X-ray holography; structure determination; X-ray fluorescence.

1. Introduction

Holography is an optical method for three-dimensional imaging of objects. The spatial resolution of the method is limited by the wavelength of radiation at which the hologram is recorded. Therefore, a large effort has been invested in the development of holographic methods at X-ray wavelengths. In the soft X-ray region, resolutions of 0.1 µm on macroscopic test objects (McNulty *et al.*, 1990) and 0.05–0.5 µm on real biological materials [see, for example, the review of Howells & Jacobsen (1990)] were achieved. At shorter X-ray wavelengths, the progress was limited by the lack of coherent radiation sources. After the arrival of third-generation synchrotron sources, the first promising experimental results were obtained at ångström wavelengths (Snigirev *et al.*, 1995).

The possibility of using X-ray fluorescence as a coherent radiation source for crystal atomic structure determination was first mentioned by Szöke (1986). Applying the idea of in-line Gabor holography, Szöke proposed the use of the fluorescence wave from an atom within the sample as a holographic reference wave R (Fig. 1*a*). This wave, scattered from the neighboring atoms, forms object waves S_i , which are fully coherent with the exciting reference wave. An interference pattern $\chi(\mathbf{k})$, interpreted as a hologram, is given in first Born approximation by

$$\chi(\mathbf{k}) = R(\mathbf{k})^2 + \sum_i R(\mathbf{k})S_i(\mathbf{k}) + \sum_{ij} S_i(\mathbf{k})S_j(\mathbf{k}), \quad (1)$$

where \mathbf{k} is the emission wavevector, and the summation is carried out over all the atoms in the object except the emitter. This interference pattern can be observed by a

detector in the far field. The square of the reference wave is angle-independent and represents a constant background. The phase information is contained in the second oscillating interference term. For objects with a long-range order, the interference of secondary waves (third term) leads to speckle patterns or Kossel lines.

The method of numerically extracting information about the positions of atoms from an experimentally recorded hologram was introduced by Barton (1988) for electrons and is based on the Helmholtz–Kirchhoff theorem. The data evaluation may be reduced to an integral that is very similar to a three-dimensional Fourier transform. The main advantage of such a method is that no preliminary information about the object is required. To suppress the ghost images that are inherent to in-line holographic methods, holograms recorded at several different energies can be used for the numerical evaluation (Barton, 1991). A comparison between the use of electrons and photons to record the holograms has been carried out (Len *et al.*, 1994; Len, Fadley & Materlik, 1997).

The first implementation of direct X-ray fluorescence holography (XFH) (Tegze & Feigel, 1996) measured strontium fluorescence from a strontium titanate single crystal over a large solid-angle. The reconstruction provided an image of the sublattice formed by the strontium atoms. The titanium and oxygen atoms were too light to be observed. The main disadvantage of XFH is the limited number of characteristic lines of the elements present in the object. This problem is solved by multiple-energy X-ray holography (MEXH) (Gog, Len *et al.*, 1996) (Fig. 1*b*), based on the idea of optical reciprocity and applying principles known from X-ray

standing waves (Bedzyk & Materlik, 1985; Gog *et al.*, 1995). MEXH uses a plane monochromatic reference wave from a source far outside the object, which excites the X-ray fluorescence. The fluorescence yield is proportional to the local intensity of the electrical field, and the fluorescing atom thus serves as detector. In addition, the incident reference wave is elastically scattered from the neighboring atoms and produces spherical object waves, which interfere with the reference wave. This interference alters the field at the position of the detecting atom. Varying the sample orientation relative to the reference wave while detecting the fluorescence yield generates a hologram at the wavelength of the incident wave. MEXH therefore allows holograms to be recorded at arbitrary energies, the main limitation being that these all lie above the absorption edge of the detecting atom. So far, MEXH has been applied to image the iron-atom positions in hematite (Gog, Len *et al.*, 1996) and Ge atoms in single-crystal germanium (Gog, Menk *et al.*, 1996).

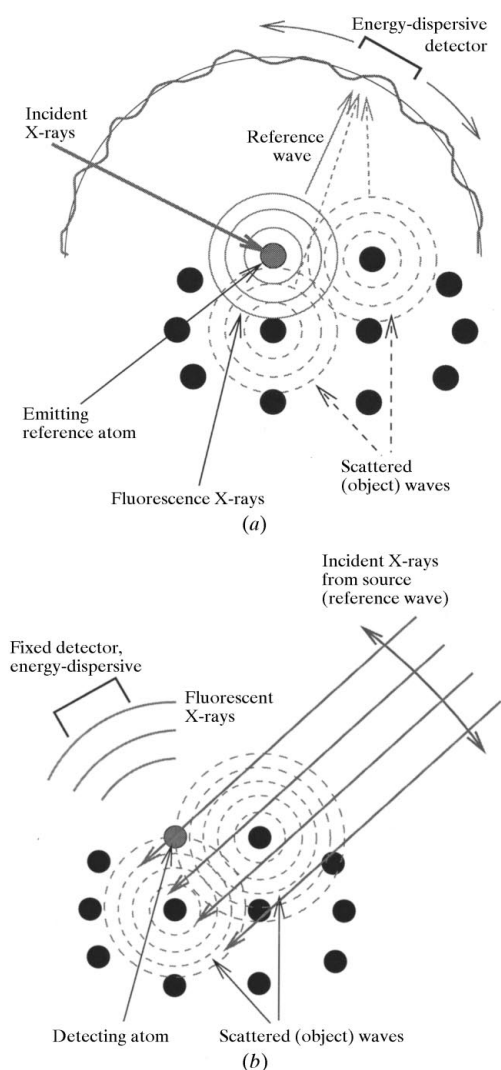


Figure 1
Formation of holograms in XFH (a) and MEXH (b) methods.

In both modifications, the atom-resolving method of X-ray holography is well suited to investigations of atomic clusters with a number of scattering centers small enough so that the third term in equation (1) stays small in relation to the second term. So far, however, all the experiments have been carried out on crystals for two reasons. First, the scattering power of atoms at X-ray wavelength is small and presently one cannot obtain a significant signal from small objects in a reasonable time. Second, this approach to X-ray holography requires objects with a long-range rotational order and a short-range translational order. Of all solid samples available easily, only crystals are suited to this requirement. The crystalline state has, however, an additional long-range translational order, which is methodically more difficult to treat for holography (Adams *et al.*, 1998). At scattering angles close to the Bragg angles of the crystal lattice, a constructive interference of secondary waves from a large number of atoms produces Kossel lines with intensities that can be much higher than the holographic signal. This high-frequency interference pattern component can be neglected far from the Bragg angles, but constrains the choice of measuring points.

For objects containing more than one fluorescent atom of the same type, the interference pattern is formed as a superposition of patterns measured independently by each detecting atom. This does not complicate the issue, provided that all detecting atoms have one and the same environment. If multiple non-equivalent positions are present, some *a priori* information is required for the interpretation of reconstructed holograms.

2. Results and discussion

In this work, the multiple-energy X-ray holography method was used for investigation of a copper oxide (cuprite, Cu_2O) single crystal. Cu_2O has a cubic ($Pn3m$) unit cell. The sample had a mosaicity of 0.2° and (111) surface orientation. The measurements were carried out at beamline BW1 at HASYLAB. The beam from the X-ray undulator source was monochromated by two Si(111) Bragg reflecting crystals and limited by 0.5×0.5 mm slits (Fig. 2). The energy of the incident beam was chosen at 11, 12 and 13 keV. The storage ring was operated in five-bunch

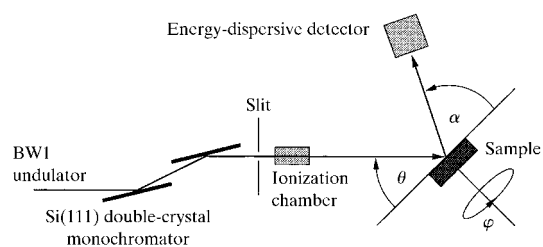


Figure 2
Experimental setup for MEXH holography measurements on a synchrotron radiation source. θ , glancing angle of the incident beam; φ , azimuthal rotation angle; α , glancing angle of the detector.

mode, and the photon flux incident on the sample was $\sim 5 \times 10^{10}$, $\sim 4 \times 10^{10}$ and $\sim 2 \times 10^{10} \text{ s}^{-1}$, respectively. The sample was placed on a multi-circle goniometer which provided rotation in a wide angular range. The energy resolving detectors were rotated together with the sample in an elevation angle θ , keeping a constant glancing angle α . For technical reasons, *i.e.* relatively large dimensions and need for fast rotation, the detectors did not follow the sample in the azimuthal angle φ .

2.1. Special requirements

The main characteristics of X-ray holography are related to the small Thomson scattering cross sections. The amplitude of a wave scattered by an electron is of the order of $r_e/r \simeq 10^{-5}$, where r_e is the classical electron radius of $2.8 \times 10^{-15} \text{ m}$ and r is the interatomic distance in solids,

$\sim 10^{-10} \text{ m}$. The scattering power of an atom is a factor of 10 higher. Thus, the contrast of the holographic signal determined by the second term in equation (1) is observed on a background, which is about four orders of magnitude stronger and is formed by the reference wave. This is rather unfavorable from the point of view of counting statistics. In order to obtain a signal larger than the statistical fluctuations of the background noise, one needs to collect at least 10^8 counts in every data point. In the direct XFH method, the dimension of the detector window defines the angular resolution of the data, leading to an obvious conflict with the necessity of getting a high flux of fluorescent photons. Reciprocal holography is free of such a limitation. The collecting angle of the detector, which is stationary relative to the sample, can be large and might in an ideal case reach 2π , the only condition being to avoid casting a shadow on the sample.

X-ray holographic measurements require an energy-resolving detection scheme since, besides fluorescence lines, other elastic and inelastically scattered photons from Bragg diffraction, diffuse and Compton scattering have to be separated. The energy resolution can be implemented either with an energy-dispersive detector (Tegze & Feigel, 1996) or with an analyser crystal in front of a detector, which can have a large dynamical range without energy resolution (Gog, Len *et al.*, 1996; Gog, Menk *et al.*, 1996). The main disadvantage of the former method is the limited dynamical range of currently existing energy-dispersive detectors, while in the latter case only a narrow solid angle is accepted.

In this work, a sixfold silicon drift detector (Lechner *et al.*, 1996), with an energy resolution of $\sim 320 \text{ eV}$ at 10 keV and at counting rates of $120 \times 10^3 \text{ counts s}^{-1}$, was used. As discussed above, the holographic signal repre-

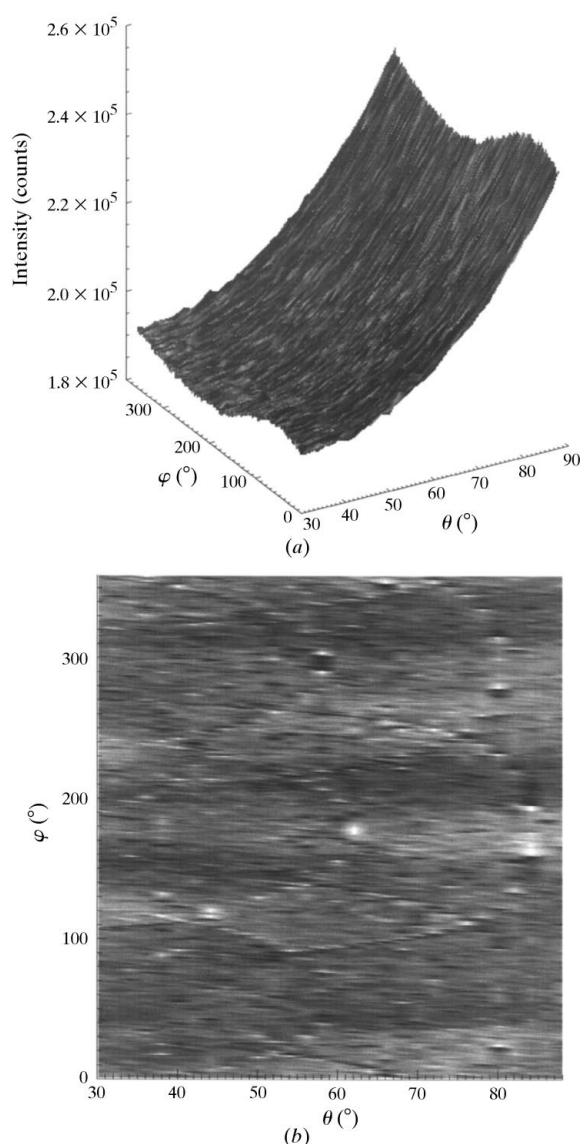


Figure 3 Experimental MEXH hologram of Cu_2O , measured in HASYLAB on BW1 at 13 keV. (a) The original data set; (b) the data set at (a) after correction for absorption.

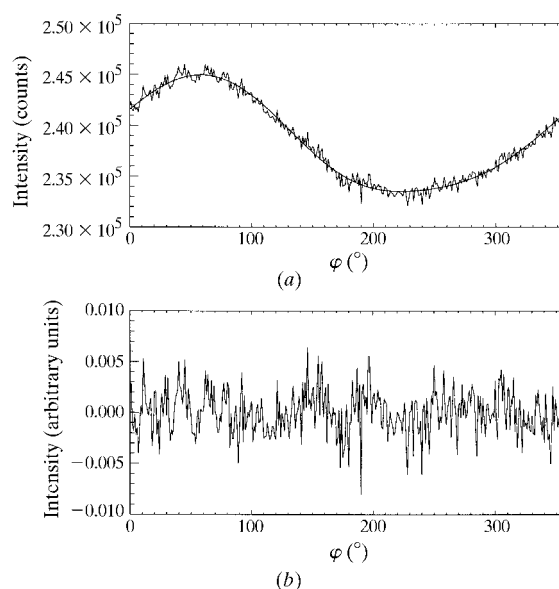


Figure 4 A singular azimuthal φ scan from the data set in Fig. 3: (a) original, (b) corrected for absorption and constant background.

sents a weak long-scale variation of intensity on a constant background.

2.2. Data treatment and image reconstruction

An original data set measured at BW1 from the Cu_2O sample at 13 keV is shown in Fig. 3(a). Although the sample surface was set normal to the φ axis with a precision of several angular minutes, the absorption of the incident and fluorescence radiation produces an emphasized sinusoidal form of the azimuthal φ scans (Fig. 4a). One can easily correct the data by fitting with the known absorption coefficients of the material (Fig. 4b). The absorption correction procedure also removes the constant background from the reference wave. Kossel lines can be clearly observed (Fig. 3b) on the resulting corrected data set.

The stationary position of the detectors relative to the sample during azimuthal scans introduces an additional artifact, which has the same nature as the holographic signal. When rotating the sample around the surface normal, one gets a MEXH hologram scan on the side of the incident beam. Simultaneously, the fluorescent radiation from the rotating sample produces, in the fixed detector, a φ scan of the direct XFH hologram. Thus, every data set measured by MEXH with a stationary detector is multiplied with an azimuthal scan of XFH.

The procedure of determination and extraction of this artifact involves additional measurements and will be presented elsewhere.

The reconstruction was carried out according to Gog, Len *et al.* (1996),

$$U(\mathbf{r}) = \int_{\mathbf{k}} dk \exp(-ik|\mathbf{r}|) \int_{\mathbf{s}} \chi(\mathbf{k}) \exp(i\mathbf{k}\mathbf{r}) k^2 \cos\theta d\theta d\varphi \quad (2)$$

where $U(\mathbf{r})$ is the X-ray electrical field distribution around the detecting atom. It can be shown that the maxima of the so-obtained $U(\mathbf{r})$ coincide with the maxima of the electron density distribution of the object (Chukhovski, 1998).

Reconstructed images of Cu_2O in the (111) plane drawn through the position of detecting copper atoms normal to the φ rotation axis for three energies separately are shown in Figs. 5(a–c). Along with atom images, artifacts from twin images, Kossel lines, sequence termination due to limited elevation angle data sets *etc.* are observed. Summation over energies suppresses most undesirable effects (Barton, 1991), leaving the images of copper atoms on the first two coordination spheres clearly resolved (Fig. 5d). Oxygen is still too light to be detected at the contrast level reached. The theoretical picture that should be given by a Cu_2O crystal, taking into account multiple nonequivalent positions occupied by copper atoms (Fig. 5e), is very similar to that obtained experimentally.

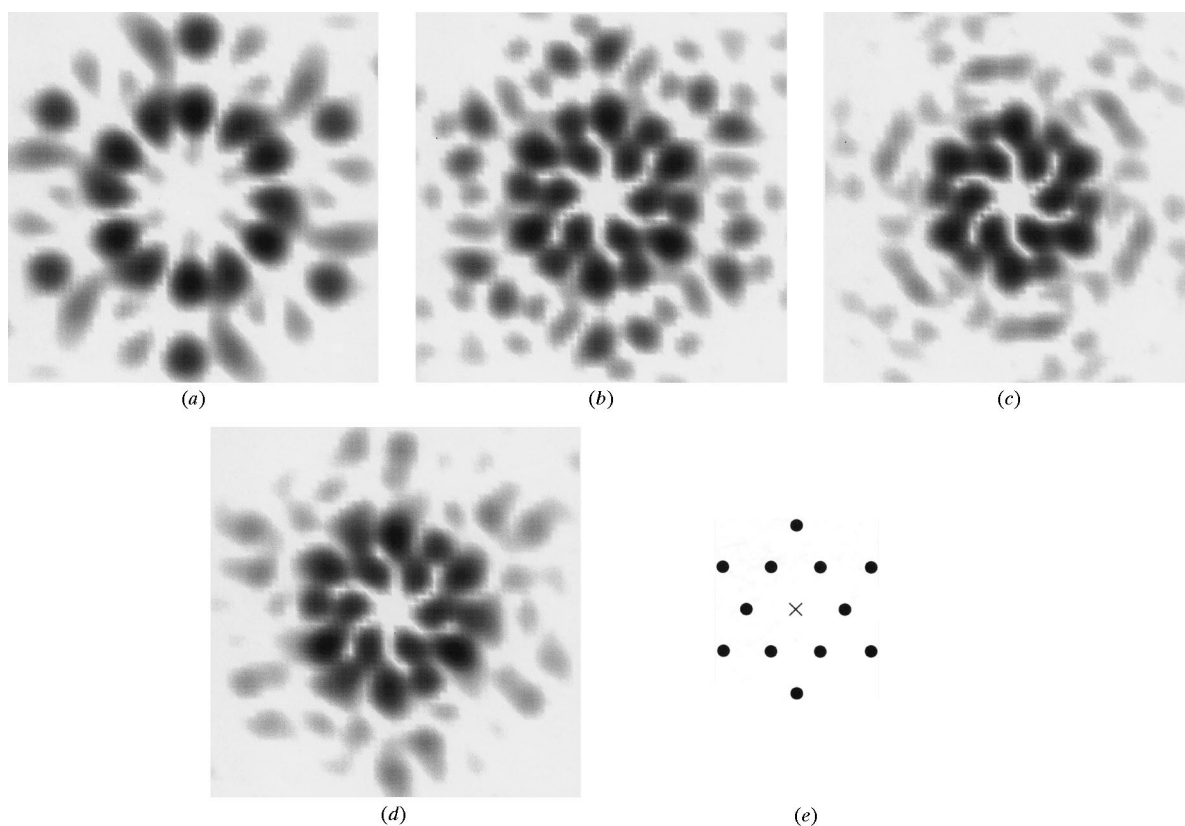


Figure 5

Reconstructed symmetrized images of the Cu_2O (111) plane, drawn through the detecting Cu atom. (a) At 11 keV; (b) at 12 keV; (c) at 13 keV; (d) summed over three energies; (e) ideal atom positions for Cu_2O ; the position of the detecting atom is marked with a cross.

3. Conclusions and outlook

In conclusion, multiple-energy X-ray holography has been implemented. For the first time, X-ray holograms were recorded at several energies to suppress artifacts during the reconstruction. Images of a Cu₂O single-crystal structure were obtained, which clearly display the first Cu–Cu coordination shells.

Further progress on the method and its practical applications requires development along three frontiers: theoretical background, data collection and data treatment technique. In the formalism used for image reconstruction, the polarization of the radiation (Adams *et al.*, 1998; Len, Gog *et al.*, 1997) has to be taken into account. The reconstruction algorithm also needs to account for near-field effects. Faster energy-dispersive detectors or multi-pixel detectors are required to reduce the data collection time and improve the data statistics, which is important for future practical applications of the method.

The authors are indebted to P. Len, T. Gog and C. Fadley for fruitful discussions, A. Sarvestani for supporting the measurements, and H.-G. Krane for furnishing the sample.

References

Adams, B., Novikov, D. V., Hiort, T. C., Kossel, E. & Materlik, G. (1998). *Phys. Rev. B*. In the press.

- Barton, J. J. (1988). *Phys. Rev. Lett.* **61**, 1356–1359.
- Barton, J. J. (1991). *Phys. Rev. Lett.* **67**, 3106–3109.
- Bedzyk, M. & Materlik, G. (1985). *Phys. Rev. B*, **32**, 6456–6463.
- Chukhovski, F. N. (1998). In preparation.
- Gog, T., Bahr, D. & Materlik, G. (1995). *Phys. Rev. B*, **51**, 6761–6764.
- Gog, T., Len, P. M., Materlik, G., Bahr, D., Sánchez-Hanke, C. & Fadley, C. S. (1996). *Phys. Rev. Lett.* **76**, 3132–3135.
- Gog, T., Menk, R.-H., Arfelli, F., Len, P. M., Fadley, C. S. & Materlik, G. (1996). *Synchrotron Radiat. News*, **9**, 30–35.
- Howells, M. R. & Jacobsen, C. J. (1990). *Synchrotron Radiat. News*, **4**, 23–28.
- Lechner, P., Eckbauer, S., Hartmann, R., Kirsch, S., Hauff, D., Richter, R., Soltau, H., Strüder, L., Fiorini, C., Gatti, E., Longoni, A. & Sampietro, M. (1996). *Nucl. Instrum. Methods*, **A377**, 346–351.
- Len, P., Fadley, C. S. & Materlik, G. (1997). *AIP Conf. Proc.* No. 389, pp. 295–319. New York: American Institute of Physics.
- Len, P., Gog, T., Novikov, D. V., Eisenhower, R. A., Materlik, G. & Fadley, C. S. (1997). *Phys. Rev. B*, **56**, 1529–1539.
- Len, P., Thevuthasan, S., Fadley, C. S., Kaduwela, A. P. & Van Hove, M. A. (1994). *Phys. Rev. B*, **30**, 11275–11278.
- McNulty, I., Kirz, J., Jacobsen, C., Anderson, E., Howells, M. R. & Rarback, H. (1990). *Nucl. Instrum. Methods*, **A291**, 74–79.
- Szöke, A. (1986). *Short Wavelength Coherent Radiation: Generation and Applications*, edited by T. Atwood & J. Boker, *AIP Conf. Proc.* No. 147, pp. 361–367. New York: American Institute of Physics.
- Snigirev, A., Snigireva, I., Suvorov, A., Kocsis, M. & Kohn, V. (1995). *ESRF Newsl.* (24), 23–25.
- Tegze, M. & Feigl, G. (1996). *Nature (London)*, **380**, 49–51.